https://doi.org/10.5194/tc-2022-75
Preprint. Discussion started: 9 June 2022

The Cryosphere Discussions

A Collection of Wet Beam Models for Wave-Ice Interaction

Sasan Tavakoli[1,2] and Alexander V. Babanin[1]

[1]Department of Infrastructure Engineering, The University of Melbourne, Parkville, 3051, VIC, Australia
[2]Department of Mechanical Engineering, Aalto University, Espoo, Finland

Correspondence: Sasan Tavakoli (sasan.tavakoli@aalto.fi)

Abstract. Theoretical models for the prediction of decay rate and dispersion process of gravity waves traveling into an integrated ice cover are introduced. The term "*wet beam*" is chosen to refer to these models as they are developed by incorporating water-based radiation forces, including heave damping and added mass, which are absent in most conventional models. Presented wet beam models differ from each other according to the rheological behavior considered for the ice cover. Two-parameter viscoelastic solid models accommodating Kelvin-Voigt (KV) and Maxwell mechanisms along with a one-parameter elastic solid model are used to describe the rheological behavior of the ice layer. Quantitative comparison between the landfast ice field data and model predictions suggests that wet beam models, adopted with both KV and Maxwell mechanisms, predict the decay rate more accurately compared to a dry beam model. Furthermore, the wet beam models, adopted with both KV and Maxwell mechanisms, are found to construct decay rates of disintegrated ice fields, though they are built for a continuous ice field. Finally, it is found that wet beam models can accurately construct decay rate curves of freshwater ice, though they cannot predict the dispersion process of waves accurately. To overcome this limitation, three-parameter solid models, termed Standard Linear Solid (SLS) mechanisms, are suggested to be used to re-formulate the dispersion relationship of wet beam models, which were seen to construct decay rates and dispersion curves of freshwater ice with an acceptable level of accuracy. Overall, the two-parameters wet beam dispersion relationships presented in this research are observed to predict decay rates and dispersion process of waves travelling into actual ice covers, though three-parameter wet beam models were seen to reconstruct the those of freshwater ice formed in a wave flume.

1 Introduction

Mutual interaction between water waves and ice is a multi-physical problem, frequently occurring in polar seas where waves can penetrate ice covers, traveling over kilometers until they die out. The phase and group speeds of the resulting gravity-flexural waves advancing through the ice can be different from that of an open-water sea owing to the effects of forces caused by solid motions. There is a pressing need to understand the mutual effects of ice and gravity waves on each other due to the recent retreat of the sea ice in the Arctic (Stroeve et al., 2008; Comiso et al., 2008; Meier et al., 2013), and the emergence of large and powerful wind-generated water waves in the Antarctic (Young et al., 2011), which can affect the ice-extent (Kohout et al., 2014) by breaking the ice. Modelers aiming to simulate wave propagation in polar regions need to use proper formulations to calculate the ice-induced energy damping and the group speed of waves traveling into ice covers (Rogers and Orzech, 2013; Liu et al., 2020).

https://doi.org/10.5194/tc-2022-75
Preprint. Discussion started: 9 June 2022

Mathematical modeling of the wave-ice interaction has first received the attentions of researchers in the 19th century. The first model was developed by Greenhill (1886), who formulated harmonic motions in a fluid domain covered with an elastic beam. To build the model, he assumed that the ice extent was spanned over an infinite way and the solid body had relatively small motions. This model lacks energy damping, but, instead, it can be employed in the prediction of the dispersion processes, the result of which is observed to be consistent with the physics of long integrated bodies covering water.

The Greenhill study is the kernel of the next generation of models established for the prediction of mutual effects of water waves and ice. Researchers looking into the wave-ice interaction developed models by modifying the original model of Greenhill. Early developments of models dating back to years between the 1950s and 1970s when scientists had become able to reach polar seas, recording the wave climate. The energy of waves traveling through the ice was observed to be reduced by sea ice (Robin, 1963; Wadhams, 1972) and the phase speed was observed to be affected by the ice. The Greenhill model lacked the former since it was developed for an elastic solid body.

Following the Greenhill's model, various mathematical models of wave-ice interaction have been developed. To address the energy decay of an integrated consolidated ice field, scholars have mostly prescribed viscoelastic behavior for the ice (*e.g.* Squire and Allan (1977); Wang and Shen (2010)) or presumed that a thin layer of viscous fluid (*e.g.* De Carolis and Desiderio (2002)) can be representative of the ice behavior. To consider the scattering of water waves by its edge, or their reflection by cracks or changes in the thickness, matching methods have been used (e.g. Fox and Squire (1991); Zhao and Shen (2013)).

Models developed for the prediction of decay rates and the dispersion process of continuously integrated ice have been developed by assuming small displacement for the cover. Thus, they solve the solid dynamic problem by using an Euler-Bernoulli beam theory. Their applications have been seen to be limited. This can be due to the reason that they have mostly developed by simplifying the problem, neglecting some aspects of the fluid and solid motions. Studies performed in the recent decade provide a clear picture of this fact. In some studies concerned with the dispersion process of waves advancing in ice (or elastic) covers, formulated dispersion relationships were reported to reconstruct the dispersion plot with an effective value of rigidity (or Young Modulus), which is much smaller than what was measured in dry tests (Langleben, 1962; Sakai and Hanai, 2002; Cheng et al., 2019). In some other studies, different values of ice viscosity were seen to give the best fitting for energy damping, which may not agree with reality (Marchenko et al. (2021)).

To overcome the limitations of available models, the role of different mechanisms in energy dissipation and the parameters influencing the dispersion process of waves propagating in ice should be understood well. Reviewing the structure of all developed models (example of review papers: Squire et al. (1995); Squire (2007); Collins et al. (2016); Squire (2020)), one can conclude that energy dissipation is either assumed to be triggered by solid motions (*e.g.* Wang and Shen (2010)) or by fluid motion, such as heave damping, overwash or shear stresses (*e.g.* Liu and Mollo-Christensen (1988); Mosig et al. (2015); Herman et al. (2019); Huang et al. (2019)). Furthermore, the dispersion process is dependent on ice rigidity in most of the models, and the effects of fluid motion on the dispersion process are rarely taken into account. All these together confirm that new models can still improved by considering the fluid-based and solid-based energy damping mechanisms at the same time. The coexistence of solid-based and fluid-based dissipation mechanisms in formulations may help us reconstruct the decay rates

https://doi.org/10.5194/tc-2022-75
Preprint. Discussion started: 9 June 2022

with fewer limitations and solve the fluid-solid problem for a more realistic condition. In addition, the ability of models in the calculation of the dispersion process can be modified by considering the effects of the viscosity of solid and fluid forces.

The present paper aims to develop wave-ice interaction models by considering fluid forces and solid forces. Distinguishing the developed models from the conventional ones, fluid forces, including heave damping and added mass are hypothesized to emerge under the elastic or viscoelastic ice layer covering water, vibrating due to the wave forces. Different solid mechanisms, linking stress and strains arising in the solid layer, are employed to establish these models. This paper is structured as follows. Models are developed in Section 2. In Section 3, results including wave height decay rates and dispersion curves are presented. At the first step, sensitivities of models to different parameters are analyzed. At the next step, predictions of models are compared against field and flume measurements. Afterward, two other patterns of rheological behavior are also used to formulate dispersion relationships. Finally, a discussion on the ability of models in the prediction of decay rates and dispersion curves is presented. In Section 4, concluding remarks and suggestions are presented.

2 Models

2.1 Development of Models

Consider a two-dimensional fluid domain containing water. The domain extend is stretched over an infinite length and has a depth of D. An ice sheet covers the upper surface of the domain. It implies that no air-water interaction occurs at all. A schematic of the domain is shown in Figure 1 (panel c). Water waves propagate in this domain and their energy is dissipated over time. Assuming that wave height is decayed exponentially, wave height at a longitudinal position of x is formulated as

$$H(x) = H_0(x)e^{-\alpha(x-x_0)}, \tag{1}$$

In Equation 1, α is the decay rate of wave height, and $H(x)$ is the wave height at $x = x_0$. In addition, as was explained in Section 1, the wavelength of ice-covered sea (the distance between two consecutive wave crests) can be different from that of open-water condition (see Figure 1 b).

Let the fluid to be ideal and irrotational. Hence, the fluid motion is represented by the potential field, which is indicated with $\Phi(\mathbf{x}, t)$. Assuming that fluid has a linear cyclic motion with a frequency of ω, the potential field can be re-written in the frequency domain, as per

$$\Phi(\mathbf{x};\mathrm{t}) = \mathrm{Re}\left[\phi(\mathbf{x})e^{i\omega t}\right]. \tag{2}$$

The Laplace Equation holds the fluid domain:

$$\nabla^2\phi(\mathbf{x}) = 0 \qquad -\infty < x < \infty \qquad -D < z < \xi. \tag{3}$$

Here, ξ is the elevation of the upper layer of the fluid domain with respect to the calm water line.

https://doi.org/10.5194/tc-2022-75
Preprint. Discussion started: 9 June 2022


The Cryosphere Discussions
Open Access
EGU

The vertical component of velocity is zero at the sea-bed, which signifies that

$$\partial_z \phi(\mathbf{x}) = 0 \qquad -\infty < x < \infty \qquad z = -D. \tag{4}$$

The solid body covering the upper layer of the water is assumed to be very thin and its thickness is denoted with h. Assuming linearity, vertical motion of the upper layer is expressed as $\mathcal{Z}(\mathbf{x};\mathrm{t}) = \mathrm{Re}\left[z(\mathbf{x})e^{i\omega t}\right]$. In the absence of fluid forces, the solid layer follows the Euler-Bernoulli beam theory, as per

$$-\omega^2 (\rho_\mathrm{i} h)\, z + \frac{G_E h^3}{6\,(1-\nu)} z^4 = p \qquad -\infty < x < \infty, \tag{5}$$

where G_E is the dynamic shear modulus of the material, which shall be introduced later. p is the wave-induced pressure, causing the vibration. The above equation is formulated for a dry beam (see panel a of Figure 1), which vibrates under the force of water waves.

In a more realistic condition, when any floating body moves due to the force of water waves, a radiation force appears, which is expressed as $f = -\omega^2 A z + i\omega \mathcal{B} z$. A and $\mathcal{B} = -B$ are respectively added mass and damping coefficients of the solid body in the vertical direction (Lamb, 1932; Newman, 1977). These two coefficients are phenomenological, related to the wave radiation potential field around the body having vertical motion (e.g. Tavakoli et al. (2020)). Also, hydrostatic force emerges when a floating body interacts with water waves. Thus, Equation 5 can be extended to

$$\left(\rho_w g - \omega^2 (\rho_\mathrm{i} h + A)\right) z - i(\omega B) z + \frac{G_E h^3}{6\,(1-\nu)} z^4 = p \qquad -\infty < x < \infty. \tag{6}$$

Equation 6 is an extended version of the Euler-Bernoulli beam model which is adopted for a beam exposed to water radiation forces. Hence, the term "wet beam" is used with an aim to distinguish the model developed based on Equation 6 from what was presented in Equation 5. The boundary condition on the fluid-solid interface is formulated as

$$\left(\rho_w g - \omega^2 (\rho_\mathrm{i} h + A)\right) (\partial_z \phi) - i(\omega B)\, (\partial_z \phi) + \frac{G_E h^3}{6\,(1-\nu)} \partial_{xxxx} (\partial_z \phi) = \rho_w \omega^2 \phi \qquad -\infty < x < \infty. \tag{7}$$

Using the separation of variable, the solution of Laplace Equation can be established as the sum of $e^{ikx}\cosh kz$. Therefore, the general form of the dispersion equation can be established as

$$k \tan(kD) = \frac{\rho_w \omega^2}{\frac{G_E h^3}{6(1-\nu)} k^4 + \rho_w g - \omega^2 (\rho_\mathrm{i} h + A) - i(\omega B)}. \tag{8}$$

As was mentioned, G_E is the shear stress modulus of the material having cyclic motions which depends on the mechanical behavior of the substance. As explained before, solid ice cover can be either assumed to be elastic or viscoelastic. As such, models have been developed for both elastic and viscolelastic ice layers. As displayed in Figure 1 d, Mechanical behaviour of these materials can be shown by using a spring (which demonstrates the elasticity nature of the material) and a dashpot (which demonstrates the viscous nature of the material).

For an elastic solid body, G_E is given by

$$G_E = G. \tag{9}$$

https://doi.org/10.5194/tc-2022-75
Preprint. Discussion started: 9 June 2022

The Cryosphere Discussions
Open Access
EGU

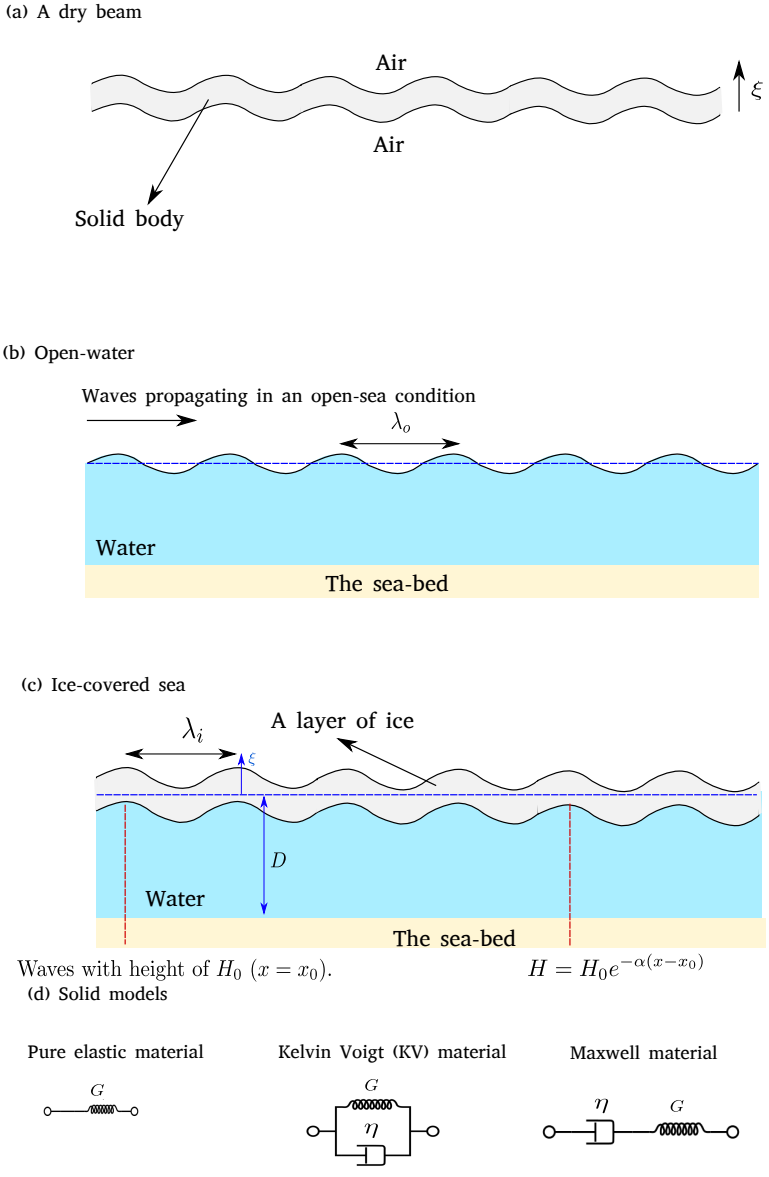

Figure 1. A pictograph of the problem and the different patterns of rheological behavior considered for the ice layer. Panel a and b repetitively show a dry beam and waves propagation in an open-water sea. Panel c shows waves propagating in an ice-covered sea. Panel d shows different rhelogical behavior that can be considered for the ice.

where G is the shear modulus of the material.

For a viscoelastic material, two different simple models can be used. The first one is Kelvin-Voigt (KV) and the second one is Maxwell. For the former, displacements of both elements (i.e. spring and dashpot) are similar, but the resulting forces are different. For a Maxwell material, however, forces emerging in elements are similar, and displacements are different.

https://doi.org/10.5194/tc-2022-75
Preprint. Discussion started: 9 June 2022

For a KV material, the dynamic shear modulus can be written as

$$G_E = G - i\omega\eta. \tag{10}$$

Here, η is the dynamic viscosity of the material (Serra-Aguila et al. (2019)). The real and imaginary parts of G_E are the storage and loss modulii. The former is responsible for harmonic response, and the latter is is responsible for energy dissipation.

For a Maxwell material, the dynamic shear modulus is given by

$$G_E = \frac{G\left(\tau^2\omega^2\right)}{(1+\tau^2\omega^2)} - i\frac{G(\tau\omega)}{(1+\tau^2\omega^2)}. \tag{11}$$

where $\tau = \eta/G$ is the relaxation time (Serra-Aguila et al. (2019)). It is worth noting that dynamic viscosity can affect the storage Modulus of Maxwell materials, and shear Modulus can affect the loss Modulus of Maxwell materials.

Dispersion relationships can be established for different materials. The first dispersion relationships is developed for water waves travelling into a pure elastic material, as

$$\omega^2 = \left(\frac{Gh^3}{6\left(1-\nu\right)\rho_w}k^4 + g - i\omega\frac{B}{\rho_w} - \frac{\rho_i(h+A)}{\rho_w}\omega^2\right)k\tanh(kD). \tag{12}$$

Another version of this relationship has been previously documented by Mosig et al. (2015), which is originally formulated by Robinson and Palmer (1990) modeled interaction of an elastic body interacting with water waves. But the added mass term is included in the above equation, which makes it different from what was presented by Mosig et al. (2015).

The second dispersion relationship describes the link between frequency and wavenumber for a KV material, which is found to be

$$\omega^2 = \left(\frac{Gh^3}{6(1-\nu)\rho_w}k^4 - i\frac{\omega\eta h^3}{6(1-\nu)\rho_w}k^4 + g - i\omega\frac{B}{\rho_w} - \frac{\rho_i(h+A)}{\rho_w}\omega^2\right)k\tanh(kD). \tag{13}$$

Finally, the dispersion relationship of a Maxwell material is formulated as

$$\omega^2 = \left(\frac{G\left(\tau^2\omega^2\right)h^3}{6(1-\nu)\left(1+\tau^2\omega^2\right)\rho_w}k^4 - i\frac{G(\tau\omega)h^3}{6(1-\nu)\left(1+\tau^2\omega^2\right)\rho_w}k^4 + g - i\omega\frac{B}{\rho_w} - \frac{\rho_i(h+A)}{\rho_w}\omega^2\right)k\tanh(kD). \tag{14}$$

Each of the above equations provides us with the roots of the dispersion relationships. We choose the dominant root with the positive real part, which refers to the wave advancing in the solid body. The dominant root is

$$k = k_i - i\alpha. \tag{15}$$

Here, k_i is the wavenumber and α is the wave decay rate which was introduced before.

2.2 Non-dimensional representation

To analyze results and to use any of the models more easily, all parameters are normalized. Parameters are normalized using the Buckingham Pi-theorem, enabling us to perform scaling law. For the first dispersion relationship, eight parameters are involved, but for the second and third relationships, nine parameters are involved. Therefore, five non-dimensional numbers

https://doi.org/10.5194/tc-2022-75
Preprint. Discussion started: 9 June 2022

are identified for the pure elastic model, and six non-dimensional numbers are identified for models developed for viscoelastic materials.

Non-dimensional numbers have been previously presented by different authors, concerted with the field wave-mud or wave-ice interaction (Jain and Mehta, 2009; Yu et al., 2019). The first non-dimensional number represents the non-dimensional wavelength in an open-water condition, which is given by

$$\hat{\lambda}_o = \lambda_o / h. \tag{16}$$

The second non-dimensional number is the non-dimensional wavenumber of waves propagating in a covered sea condition, given by

$$\hat{k}_i = k_i / k_o. \tag{17}$$

The attenuation rate is normalized as

$$\hat{\alpha}_i = \alpha / k_o. \tag{18}$$

The third non-dimensional number is the elasticity per unit of mass, which can be formulated as

$$\hat{G} = G / \rho_i g h. \tag{19}$$

In the present research, $\hat{G}$ is called Elasticity number (which is inspired by Yu et al. (2019)). The other non-dimensional number is

$$\hat{\eta} = \eta / \rho_i \sqrt{g h^3}. \tag{20}$$

The fourth non-dimensional number is the relative density of the ice, and is calculated by

$$\hat{\rho} = \rho_i / \rho_w. \tag{21}$$

The hydrodynamic damping coefficient is normalized by

$$\hat{B} = B / \rho_w \sqrt{g h}. \tag{22}$$

The added mass coefficient can be normalized by

$$\hat{A} = A / \rho_w h^2. \tag{23}$$

Note that the added mass and damping coefficients are assumed to be two-dimensional.

3 Results and discussions

Results of wet beam models are presented in five separate sub-sections. The first sub-section presents a discussion on the effects of different parameters on the dispersion and decay rate plots. The primary aim is to provide a better understanding

https://doi.org/10.5194/tc-2022-75
Preprint. Discussion started: 9 June 2022

of the sensitivity of models to mechanical behavior of material and fluid forces. The second and third sub-sections discuss the ability of models in reconstruction of the decay rate and dispersion process through comparing their results against field and flume measurements. A brief summary of these measurements is documented in Table 1. In the fourth sub-section it is attempted to understand whether any other solid model can be used to formulate the dispersion relationship or not. Final sub-section of results presents a deep discussion on models and their abilities with covering limitations of models.

3.1 Effects of different parameters on decay rate and dispersion process

Figure 2 shows the normalized decay rates calculated by setting different values for the mechanical properties of the cover. The first, second and third columns respectively show the data found for KV, Maxwell, and pure elastic materials. The first and second rows show the effects of dynamic viscosity on energy decay. The results presented in the first row correspond to a material with $\sqrt{\hat{G}} = 340$ and the ones plotted in the panels of second row correspond to a material with $\sqrt{\hat{G}} = 3.4$.

As seen, for a viscoelastic material with a larger rigidity, $\hat{\alpha}$ increases with the increase in $\hat{\lambda}_o$ reaching a maximum value at a critical wavelength. With the increase in $\hat{\lambda}_o$, $\hat{\alpha}$ decreases. For a KV material, the critical $\hat{\lambda}_o$ is sensitive to the dynamic viscosity, growing with the increase in the dynamic viscosity. For a Maxwell material, the increase in the dynamic viscosity reduces the decay rate. Interestingly, the pure elastic model gives negligible decay rates at small dimensionless wavelengths ($\hat{\lambda}_o < 50$). The decay rates of a pure elastic material peaks at a specific $\hat{\lambda}_o$. It is worthy to note that the dimensionless fluid damping used to calculate the decay rates is set to be 0.0032.

To provide a clear picture of the effects of the fluid damping on the decay rates, $\hat{\alpha}$ vs. $\hat{\lambda}_o$ curve the pure elastic model gives is plotted in the first and second columns (dashed curve). Interestingly, the decay rates of the viscoelastic materials converge to that of the pure elastic model, signifying that the contribution of solid-based energy dissipation vanishes at relatively long waves. Instead, the fluid-based energy damping becomes dominant over the range of long waves.

Now we discuss the decay rates of covers with a lower rigid (second row). No critical $\hat{\lambda}_o$ is observed in $\hat{\alpha}$ vs. $\hat{\lambda}_o$ curves the KV model gives for a low Elasticity number. Decay rate of KV model with low rigidity reduces with an increase in dimensionless wavelength. The increase in the dynamic viscosity can affect the decay rate, though its effects are noticeable at shorter waves. For longer waves, however, different values of $\hat{\eta}$ give similar decay rates, which match with the those of a pure elastic material. This matches with what was observed for the larger rigidity (upper row). For a Maxwell material with low

Table 1. Cases studied in the present paper.

Reference	Type of cover	Type of test
Voermans et al. (2021)	Landfast ice covers (Arctic and Antarctic)	Field measurement
Wadhams et al. (1988)	Unconsolidated ice field (Greenland Sea)	Field measurement
Meylan et al. (2014)	Unconsolidated ice field	Field measurement
Yiew et al. (2019)	Freshwater ice cover	Flume measurement
Sree et al. (2018)	Viscoleastic cover	Flume measurement

https://doi.org/10.5194/tc-2022-75
Preprint. Discussion started: 9 June 2022

rigidity, a critical $\hat{\lambda}_o$ emerges over the short wavelength range. Similar to KV materials, the decay rate of Maxwell materials with low rigidity are sensitive to the dynamic viscosity over a very short range of wavelengths. The $\hat{\alpha}$ vs. $\hat{\lambda}_o$ curves found by setting different values for the dynamic viscosity converge to each other and finally aligned to the decay rates of pure model. This again confirms that fluid-based energy damping becomes dominant with the increase in the dimensionless wavelength.

The last row of Figure 2 compares the decay rates of materials with different Elasticity numbers. As apparent, when a KV model is used, an increase in Elasticity number reduces the decay rate. The most significant effects of elasticity on decay rate emerge at short wavelengths, where the solid-based energy damping is expected to be dominant. The decay rates of KV materials with different Elasticity numbers converge to those of the pure elastic material. The decay rate of a Maxwell material is proportional to its elasticity. Similar to decay rate plots of KV materials with different Elasticity numbers, decay rates of Maxwell materials with different Elasticity numbers converge to what the pure elastic model predicts.

Figure 3 shows how the consideration of fluid damping can affect the decay rates. Three different plots are presented, each of which shows the decay rates found by setting different values for the heave damping coefficient. The solid blue curves show the data found by setting a zero heave damping, *i.e*, this plot represents the decay rates calculated in the absence of fluid damping. The two other plots show the decay rates predicted by setting two different values for the heave damping coefficient.

The left panel of Figure 3 shows the data related to a KV material. As apparent, when the fluid damping coefficient is set to be zero, the decay rate decreases with a very high rate at $\hat{\lambda}_o > 180$. By assuming a non-zero value for the heave damping coefficient, one abrupt reduction in $\hat{\alpha}$ vs. $\hat{\lambda}_o$ curve occurs, though the rate of the reduction of the decay rate as a function of the dimensionless wavelength decreases with the increase in the wavelength. Eventually the decay rate decreases with a mild rate over the range of $\hat{\lambda}_o > 400$. This confirms that the fluid-based energy damping becomes dominant over this range. For a large fluid-damping coefficient, as seen, the sudden reduction in the decay rate does not occur, and decreases with a low rate after reaching its peak value.

The decay rates of a Maxwell material with considering different heave damping are plotted in the right panel. Trends of the presented curves are consistent with the ones observed in the left panel of Figure 3 (KV material). This demonstrates that the effects of fluid-damping on decay rates are insensitive to the nature considered for materiel, which matches with the presented formulations for the dispersion relationships.

The dispersion relationships are also employed to calculate wavenumbers of waves propagating into viscoelastic covers. Results are depicted in Figure 4. The density of covers is set to be $\rho_i/\rho_w = 0.9$ which is very close to that of the sea ice. The two upper panels of Figure 4 show the dimensionless wavenumbers found for KV materials with different Elasticity numbers. Zero heave added mass coefficients (solid curve) and two none-zero heave added mass coefficients are considered.

As apparent, when the Elasticity number of a KV material is greater (left) and the heave added mass is nil, the dimensionless wavenumber is below 1.0 at small values of $\hat{\lambda}_o$. This means that, compared to an open-sea condition, gravity waves travailing into a solid cover becomes longer over the range of short open-water wavelength. $\hat{k}_i$ increases with the increase in $\hat{\lambda}_o$. and eventually converges into 1.0, where plotted curves are flattened out, meeting the reference line (the dashed blue line). Interestingly, the contribution of the heave added mass coefficient to the dispersion process in the covered sea can affect the wavenumber. Under the action of heave added mass forces, wavenumber becomes greater. The effects of heave added mass on

https://doi.org/10.5194/tc-2022-75
Preprint. Discussion started: 9 June 2022

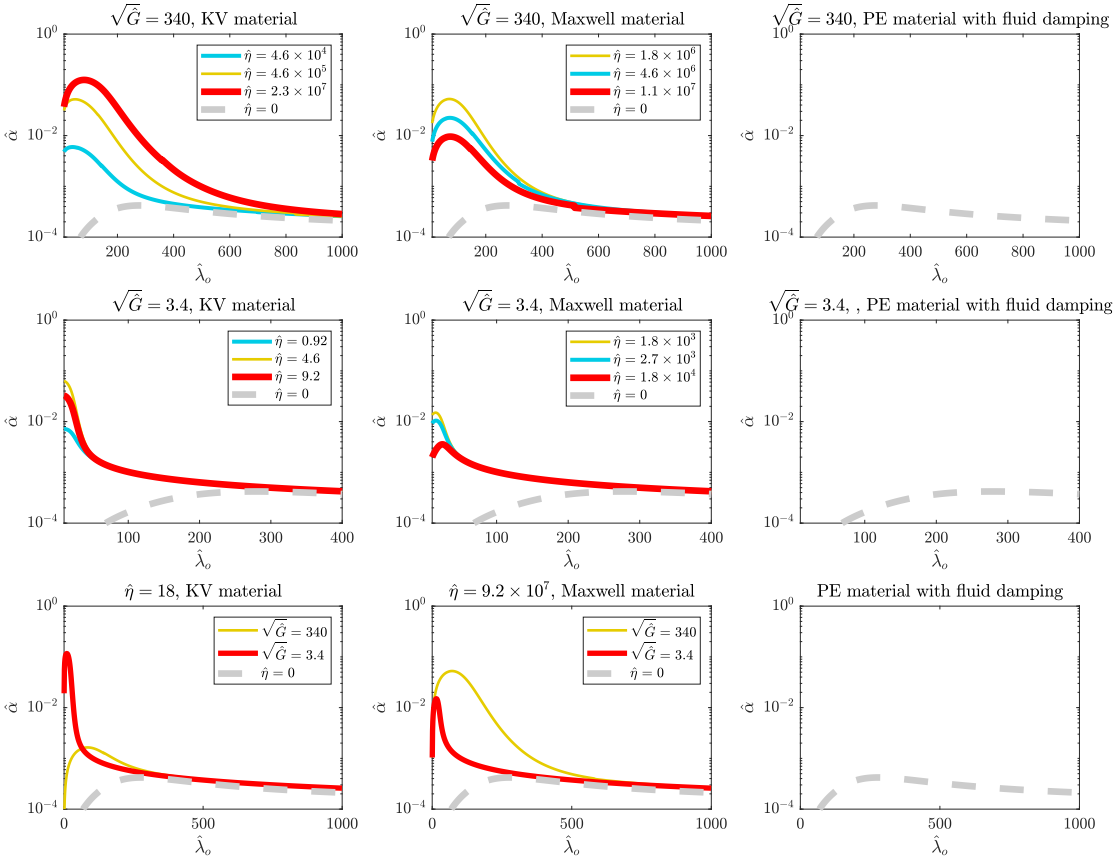

Figure 2. Effects of the dynamic viscosity (upper and middle rows) and Elasticity number (lower row) on $\hat{\alpha}$ vs. $\hat{\lambda}_o$ curves different solid models give.

the wavenumber are more significant over $100 < \hat{\lambda}_o < 600$. When the heave added mass coefficient is set to be very large, the dimensionless wavenumber becomes greater than 1.0, reaching a maximum value and then decreases, converging into 1.0.

For a KV material with low density and a zero heave added mass coefficient, the wavenumber is below 1.0 when the dimensionless open-water wavelength is small. Compared to a KV material with a greater Elasticity number (left panel), $\hat{k}_i$ becomes lower than 1.0 over a narrower range of $\hat{\lambda}_o$. This implies that waves propagating into a solid cover are lengthened over a wider range of dimensionless open water wavelength when rigidity increases. $\hat{k}_i$ becomes greater than 1.0 and reaches a peak value over the range of short the open-water wavelength ,which is in contrast with what was observed for material with a larger Elasticity number and zero heave added mass (left panel).

https://doi.org/10.5194/tc-2022-75
Preprint. Discussion started: 9 June 2022

The Cryosphere Discussions
Open Access
EGU

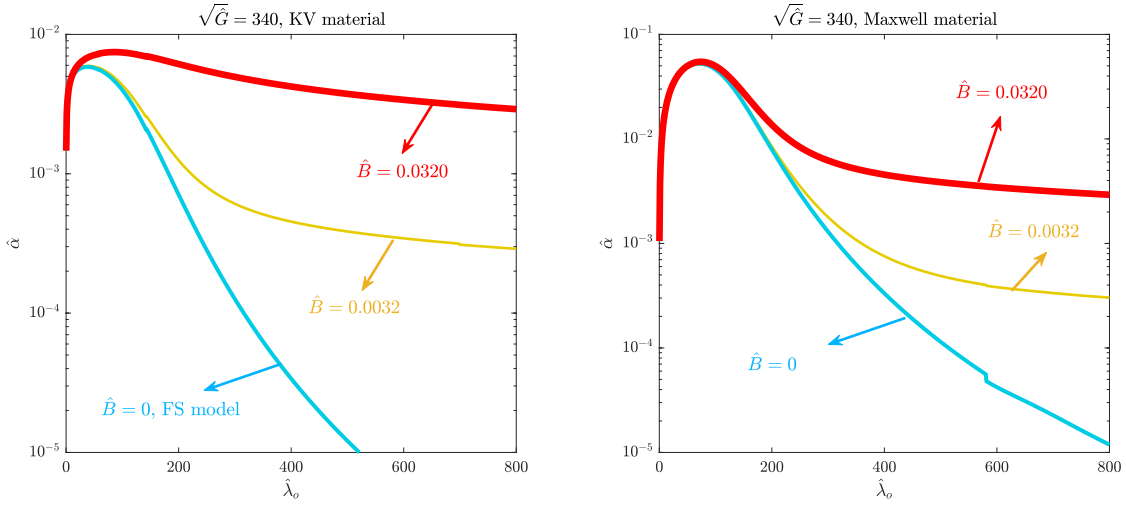

Figure 3. Effects of heave fluid damping on $\hat{\alpha}$ vs. $\hat{\lambda}_o$ curves viscoelastic models give.

The heave added mass coefficient is seen to affect the dispersion process of waves propagating into the cover with lower rigidity, which matches with what was observed for the cover with large rigidity (left panel). But the heave added mass coefficient can affect the wavenumber of waves travelling through the solid cover more noticeably when rigidity is lower.

The two lower panels of Figure 4 show the calculated dimensionless wavenumbers of gravity waves propagating into a solid cover hypothesized to behave in the same way Maxwell materials do. Left and right panels respectively show the curves corresponding to covers with relatively large and low Elasticity numbers. The trends of curves plotted in the left panel confirm that the dynamic viscosity can slightly affect the wavenumber of waves advancing in the cover with a large Elasticity number. The influence of dynamic viscosity on wavenumber is not significant and emerges over a relatively narrow range, (the close-up view provides the evidence). Dimensionless wavenumber is seen to be insensitive to the dynamic viscosity of Maxwell materials when Elasticity number is low (right panel).

3.2 Ability of models in prediction of the decay rates

Decay rates of two recent field tests are presented in Figure 5 (circle markers). Upper and lower rows respectively display the data corresponding to field tests took place in Arctic and Antarctic. The first, second, and third columns of Figure 5 respectively show the decay rates predicted by prescribing Kelvin-Voigt, Maxwell, and pure elastic materials. The decay rates found by setting zero heave damping coefficient are also plotted to demonstrate how the inclusion of the fluid damping can improve the accuracy of models in the prediction of the decay rates.

Viscoelastic models cannot follow the field data when fluid heave damping is set to be zero, and tails of curves diverge from that of the field data. This can be seen in both upper and lower rows of Figure 5. In this condition, the increase of the dynamic viscosity cannot affect the trend of $\hat{\alpha}$ vs. $\hat{\lambda}_o$, and may only shift the curve upward or downward, depending on the

https://doi.org/10.5194/tc-2022-75
Preprint. Discussion started: 9 June 2022

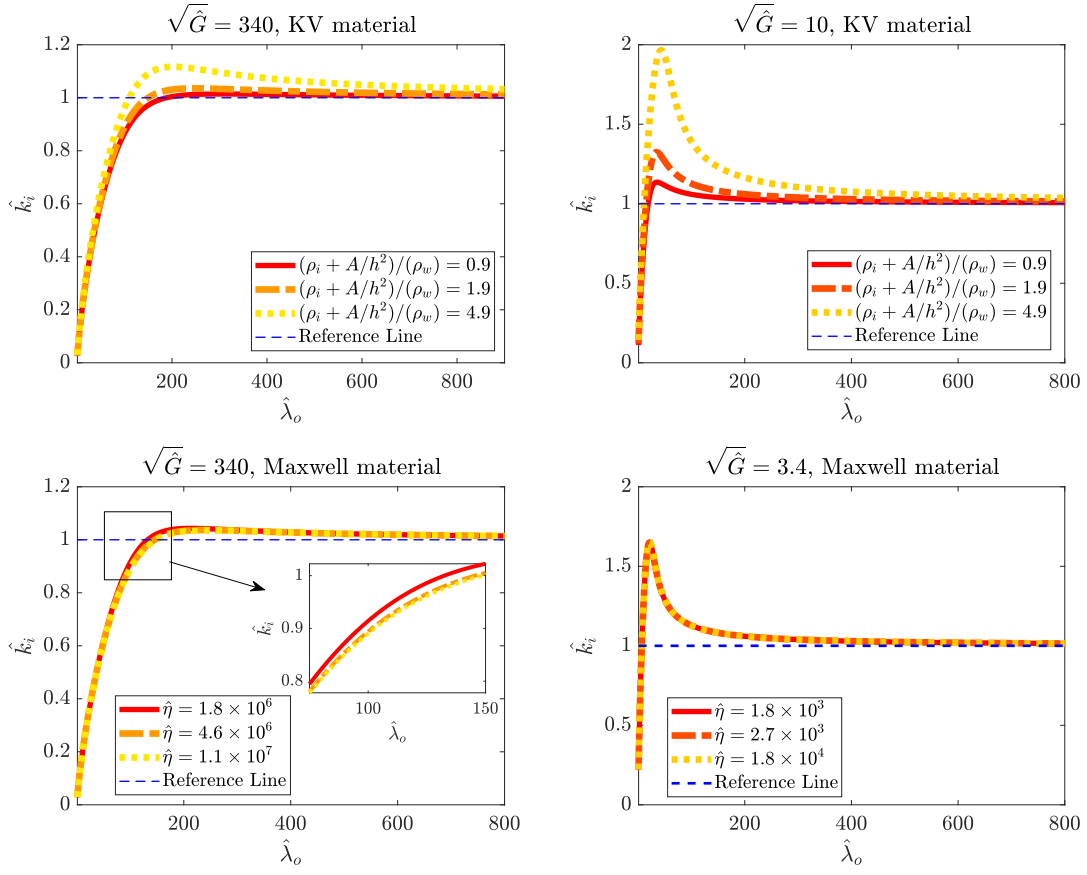

Figure 4. Effects of the added mass force (upper row) and the dynamic viscosity (lower row) on the dispersion curves of waves propagating in an ice-cover.

nature considered for the material. But, when the fluid damping coefficient is set to be non-zero, the $\hat{\alpha}$ vs. $\hat{\lambda}_o$ follow the field data. This confirms that heave damping can contribute in energy damping occurring under a landfast ice cover. Interestingly, heave damping coefficients used to predict the decay rates of viscoelastic are similar.

For the KV material, a dynamic viscosity of $1.3 \times 10^8 Pa.s$ gives the best fitting for both ice covers. But for a Maxwell material, a dynamic viscosity of $4.4 \times 10^{10} Pa.s$ gives the best fitting. Finally, the pure elastic material assumption can also be used to fit curves with the field experiments. But, compared to KV and Maxwell models, a greater value of heave fluid damping gives the best fitting for an elastic model.

The decay rates of two different broken ice fields are calculated using the wet beam models and are compared against measurements. Field data and calculated decay rates are plotted in Figure 6. The data presented in upper and lower panels of this Figure are respectively documented in Wadhams et al. (1988); Meylan et al. (2014).

https://doi.org/10.5194/tc-2022-75
Preprint. Discussion started: 9 June 2022

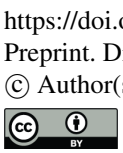

The Cryosphere Discussions
Open Access
EGU

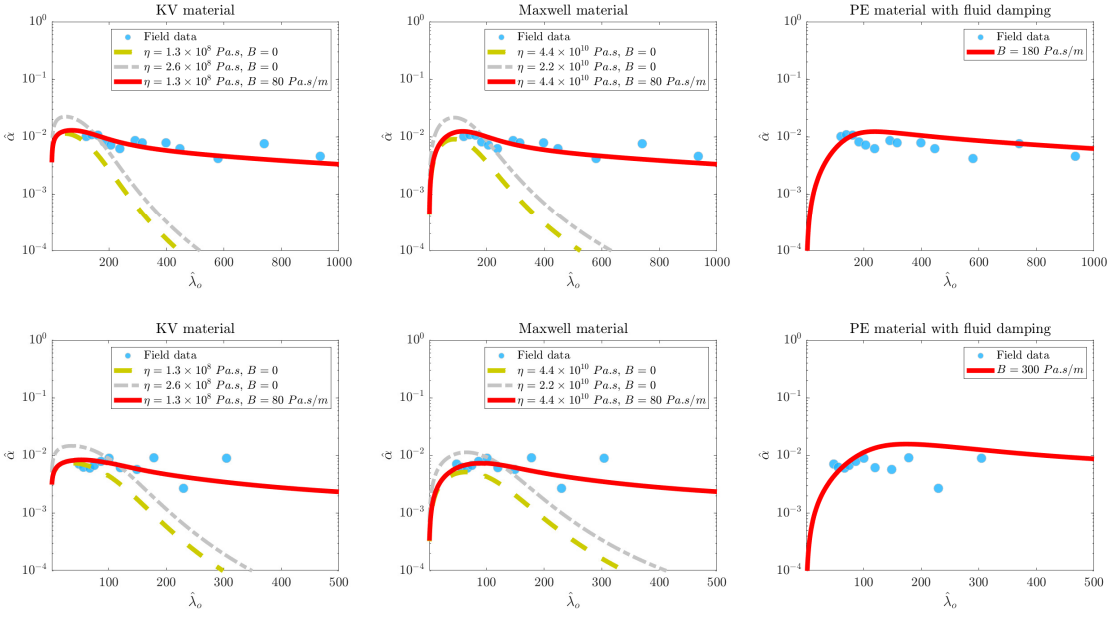

Figure 5. Comparisons between $\hat{\alpha}$ vs. $\hat{\lambda}_o$ curves predicted by different models and the data measured by Voermans et al. (2021). Upper and lower rows respectively show data measured in Arctic and Antarctic. In the first and second columns, decay rates predicted by setting a zero heave damping are also plotted. The shear Modulus of ice is set to be 1 GPa.

Wet beam models established for viscoelastic materials can predict decay rate curves of broken ice field with a good level of accuracy when heave damping is incorporated in calculations. Similar to curves plotted in Figure 5, increase or decrease in the dynamic viscosity of the material can shift the curves vertically, not affecting the tail of $\hat{\alpha}$ vs. $\hat{\lambda}_o$ curve. The curve given by a pure elastic material is not accurate at all dimensionless wavelengths. This implies that to accurately compute the decay rate of a broken ice field, solid-based energy damping caused by the viscoleastic behaviour of the solid needs to be taken into consideration which is being lacked in a pure elastic model.

Wet beam models are employed to calculate the decay rates of waves traveling into viscoelastic covers, with an aim to understand whether they can be used to predict attenuation rates measured in flume tests or not. The reconstructed $\hat{\alpha}$ vs. $\hat{\lambda}_o$ curves are presented in Figure 7. The upper and lower rows show the data corresponding to covers with low and large rigidity.

The curves reconstructed by viscoelastic models cannot follow the experimental data if the fluid damping is not considered. Dashed and dashed-dotted curves plotted in the first and second columns provide shreds of evidence. Their results only match with experimental data at very small dimensionless open-water wavelengths. Viscoelastic-based models can accurately predict decay rates when the fluid damping is set to be non-zero. The elastic model can calculate decay rates with an acceptable level of accuracy. The fluid heave damping that gives the best fitting for pure elastic material is slightly greater than those of models built for viscoelastic materials.

https://doi.org/10.5194/tc-2022-75
Preprint. Discussion started: 9 June 2022

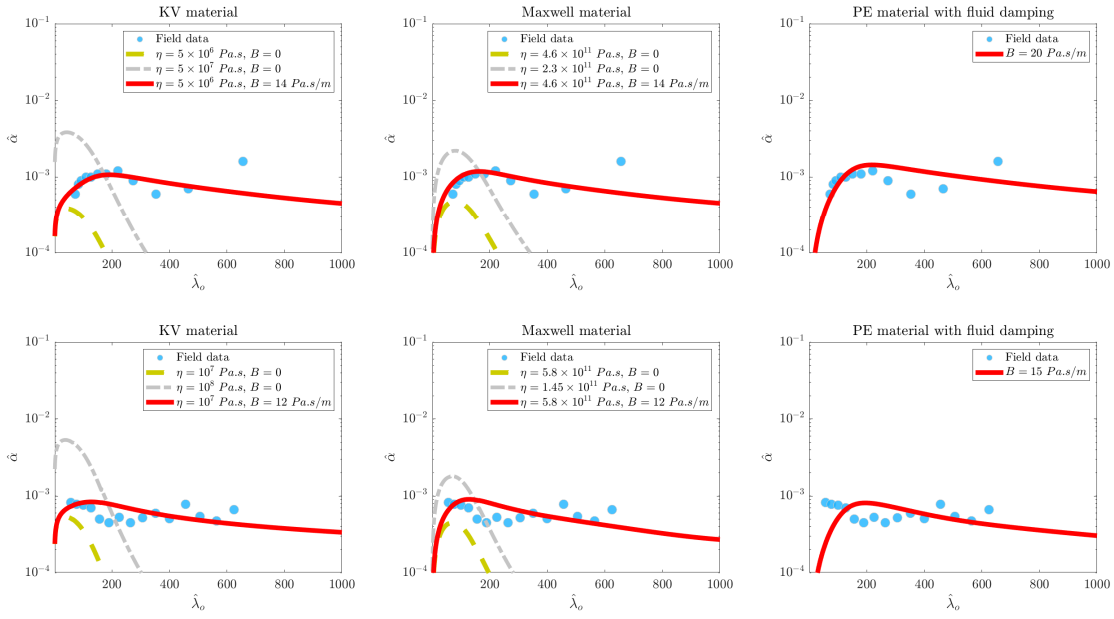

Figure 6. Comparisons between $\hat{\alpha}$ vs. $\hat{\lambda}_o$ curves predicted by different models and the data measured by by Wadhams et al. (1988), upper row, and Meylan et al. (2014), lower row. In the first and second columns, decay rates predicted by setting a zero heave damping are also plotted. The shear Modulus of ice is set to be 1 GPa.

At the final stage, the decay rates of the freshwater ice formed in the wave flume of the University of Melbourne are predicted by using the presented models. Figure 8 displays the decay rates plots and experimental data. The results presented in the upper and lower rows of Figure 8 are related to 1 cm and 1.5 cm thick ice covers. Before conducting flume experiments, Parra et al. (2020) measured the Young Modulus of the dry freshwater ice, reporting that Young Modulus is nearly 3 GPa.

The KV model can accurately predict the decay rates of 1 cm thick ice when dynamic viscosity is set to be 2.6×10^9 $Pa.s$. Inclusion of the heave fluid damping is seen to be ineffective when KV model is used. The Maxwell model can also predict the decay rate curve of the 1 cm thick ice cover with a good level of accuracy. But the decay rates Maxwell model predicts depend on the fluid heave damping. The model developed for pure elastic materials can construct $\hat{\alpha}$ vs. $\hat{\lambda}_o$ curve if fluid damping is set to be 1300 $Pa.s/m$, which is as 13 times greater than those considered for KV and Maxwell models. This significant difference between heave damping of pure elastic model and viscoelastic models, which was never observed in previous Figures, indicating that the solid-based damping highly contributes to energy dissipation over the range of tested waves in the laboratory. To compensate the absence of the solid-based energy damping of the pure elastic model, a very large heave damping needs to be used. This is in contrast with what was observed for the tests of Sree et al. (2018), where the difference between fluid heave damping of elastic and viscoelastic models was not significant. The big difference between the Elasticity numbers of the covers tested by Sree et al (2018) and ice covers tested by Yiew et al. (2019) explains this behavior.

https://doi.org/10.5194/tc-2022-75
Preprint. Discussion started: 9 June 2022

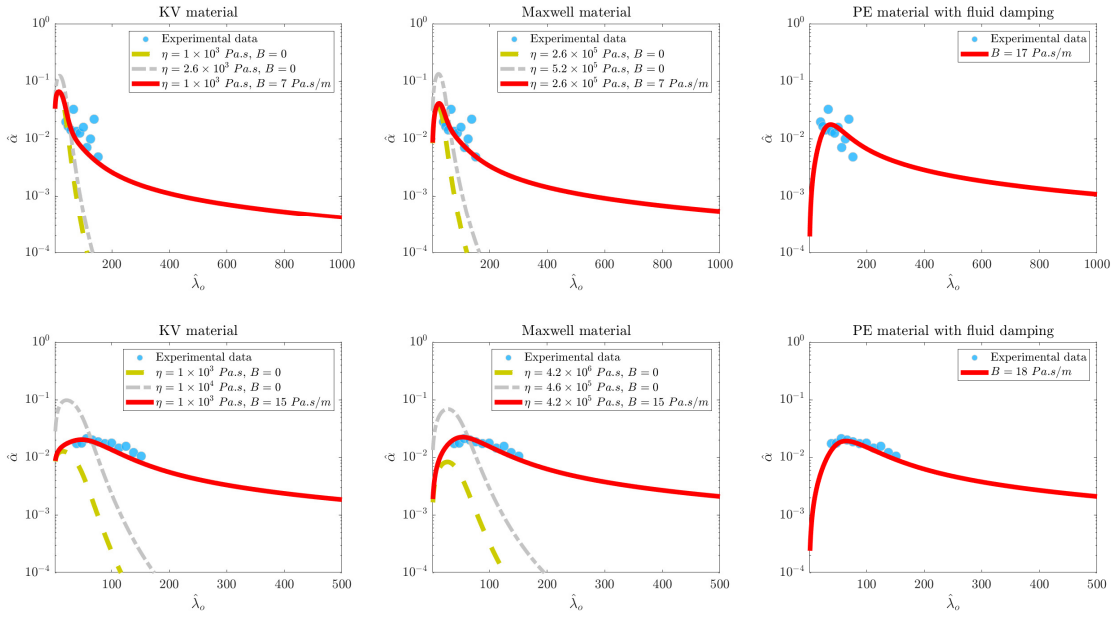

Figure 7. Comparison between $\hat{\alpha}$ vs. $\hat{\lambda}_o$ curves predicted by models and the data measured by Sree et al. (2018). Upper and lower rows show the data related to a cover with a shear Modulii of 20 KPa and 80 KPa respectively.

It was also demonstrated that when Elasticity number is low, the solid-based energy damping contributes to energy dissipation over a narrow range of wavelengths (second row of Figure 2), compared to a cover with a larger Elasticity number (first row of Figure 2).

The KV model under-predicts the decay rate curve of 1.5 cm thick ice cover irrespective of the values of the dynamic viscosity and the fluid heave damping coefficients. The Maxwell model, however, can construct $\hat{\alpha}$ vs. $\hat{\lambda}_o$ curve when a dynamic viscosity value of 4×10^6 $Pa.s$ is set. This value is lower than that the dynamic viscosity gave the best fitting for the thinner ice. Artificial effects, boundary conditions, and the presence of side walls may cause a larger energy damping pattern when fluid interacts with the thicker ice (Sutherland et al., 2016). Thus, different values of dynamic viscosity give the best fitting for 1 cm and 1.5 cm thick ice covers. It is important to note that dynamic viscosity values giving the best fitting for the landfast ice were not seen to be different (Figure 5), where artificial effects are less likely to contribute. As seen, fluid heave damping does not have any significant effect on the curve over the range of tested waves. It can only affect the tail of curve. This again confirms that the solid-based energy damping is dominant over the range of tested waves. If tests covered a wider range of open-water wavelengths, especially longer ones, a proper value for fluid damping could be found through fitting predicted curves with experimental data. When the pure elastic model is used to calculate decay rates, a very large heave fluid damping needs to be set, but the curve can never meet the experimental data.

https://doi.org/10.5194/tc-2022-75
Preprint. Discussion started: 9 June 2022

The Cryosphere Discussions
Open Access
EGU

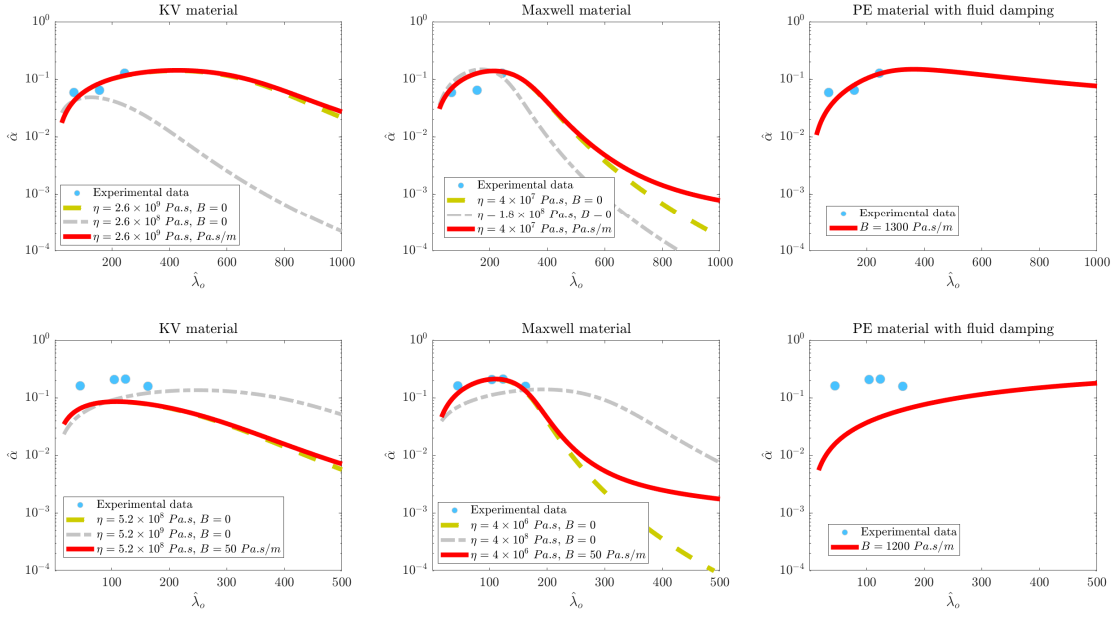

Figure 8. Comparison between $\hat{\alpha}$ vs. $\hat{\lambda}_o$ curves predicted by models and the data measured by Yiew et al. (2019). Upper and lower rows show the data related to freshwater ice covers with thicknesses of 1 cm and 1.5 cm, respectively.

3.3 Ability of models in the prediction of the dispersion process

The accuracy of models in the calculation of the dispersion process of waves travelling through viscoelastic covers is also evaluated. First, the dispersion curves of waves propagating into landfast ice are constructed, and then the dispersion curves of waves advancing in freshwater ice are plotted.

Figure 9 shows the normalized wavenumber $\hat{k}_i$ vs. $\hat{\lambda}_o$ curves of landfast ice. Symbols indicate the field measurements and curves denote the calculated dimensionless wavenumbers. Left and right panels repressively show predictions made for Maxwell and KV materials. As seen, both models can predict the dispersion process of waves traveling into the landfast ice with an acceptable level of accuracy. The inputs that are used for the construction of dispersion curves are similar to what gives the best fitting for decay rates.

Figure 10 shows the $\hat{k}_i$ vs. $\hat{\lambda}_o$ plots of the flume tests performed in University of Melbourne. It was observed that none of the models can predict the dispersion process of waves interaction with freshwater ice with the inputs gave the best fitting for the decay rates plots (Figure 8). This is in contrast with what was observed in Figure 9, where models accurately predicted the wave dispersion process with similar inputs utilized for the calculation of decay rates. As seen, when dispersion process of waves interacting with freshwater is constructed by using a KV model, Young Modulus values of 5×10^5 Pa and 2.5×10^8 Pa give the best fitting for the dispersion processes of 1 cm and 1.5 cm ice covers, respectively . As explained in the literature, some

https://doi.org/10.5194/tc-2022-75
Preprint. Discussion started: 9 June 2022

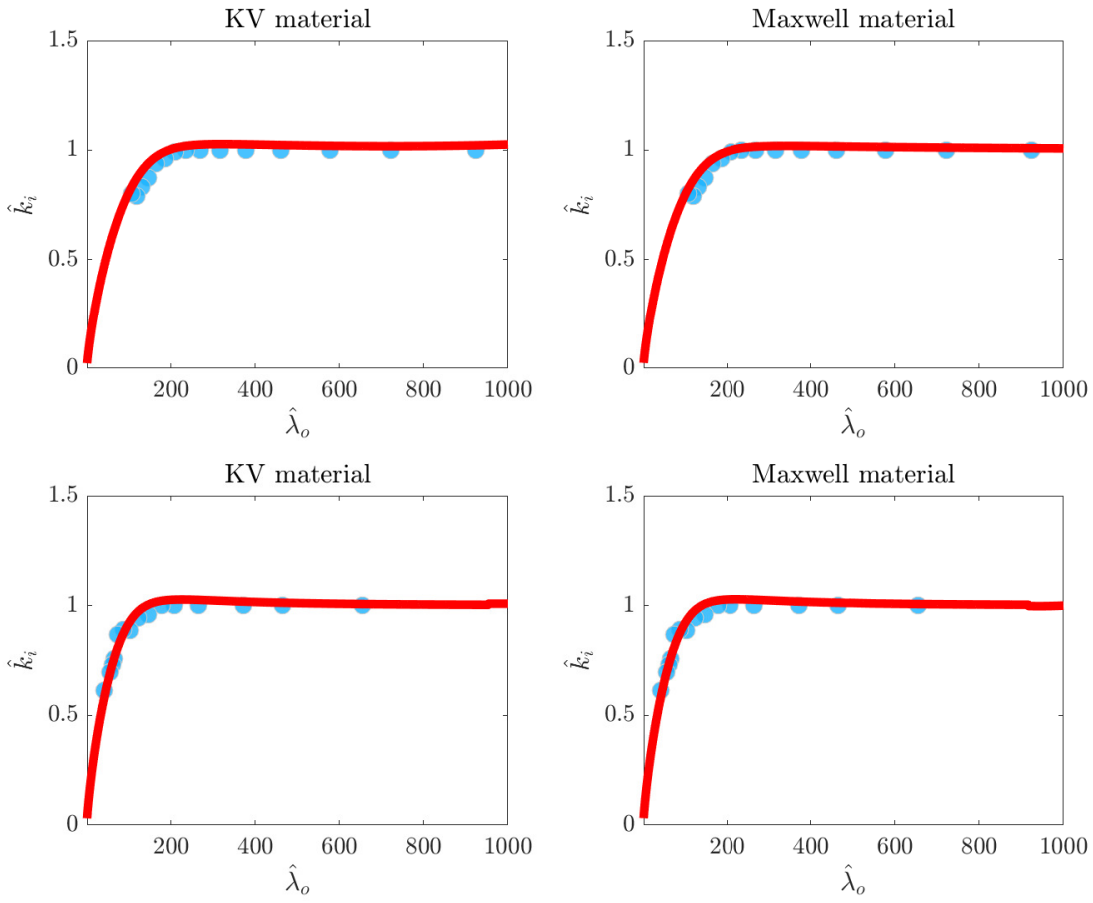

Figure 9. Comparison between $\hat{k}_i$ vs. $\hat{\lambda}_o$ curves predicted by wet beam models and the data measured by Voermans et al. (2021). Upper and lower rows respectively show data related to tests performed in Arctic and Antarctic. The shear Modulus of ice is set to be 1 GPa.

other researchers observed that the effective Young Modulus of a material is different and smaller from what is measured in dry tests. For a Maxwell material, however, different values of dynamic viscosity can be used to fit the curves with the experimental data. It was previously demonstrated that the dynamic viscosity can affect $\hat{k}_i$ vs. $\hat{\lambda}_o$ plots by increasing the wavenumber over the range of short waves. By setting larger values for the dynamic viscosity, the constructed dispersion curve matches with the experimental data (the solid curve).

3.4 Other models

In sub-sections 3.2 and 3.3, it was observed that proposed models cannot accurately calculate the dispersion process and decay rates of waves advancing into the freshwater ice. Artificial effects may have contributed to the dispersion and dissipation

https://doi.org/10.5194/tc-2022-75
Preprint. Discussion started: 9 June 2022

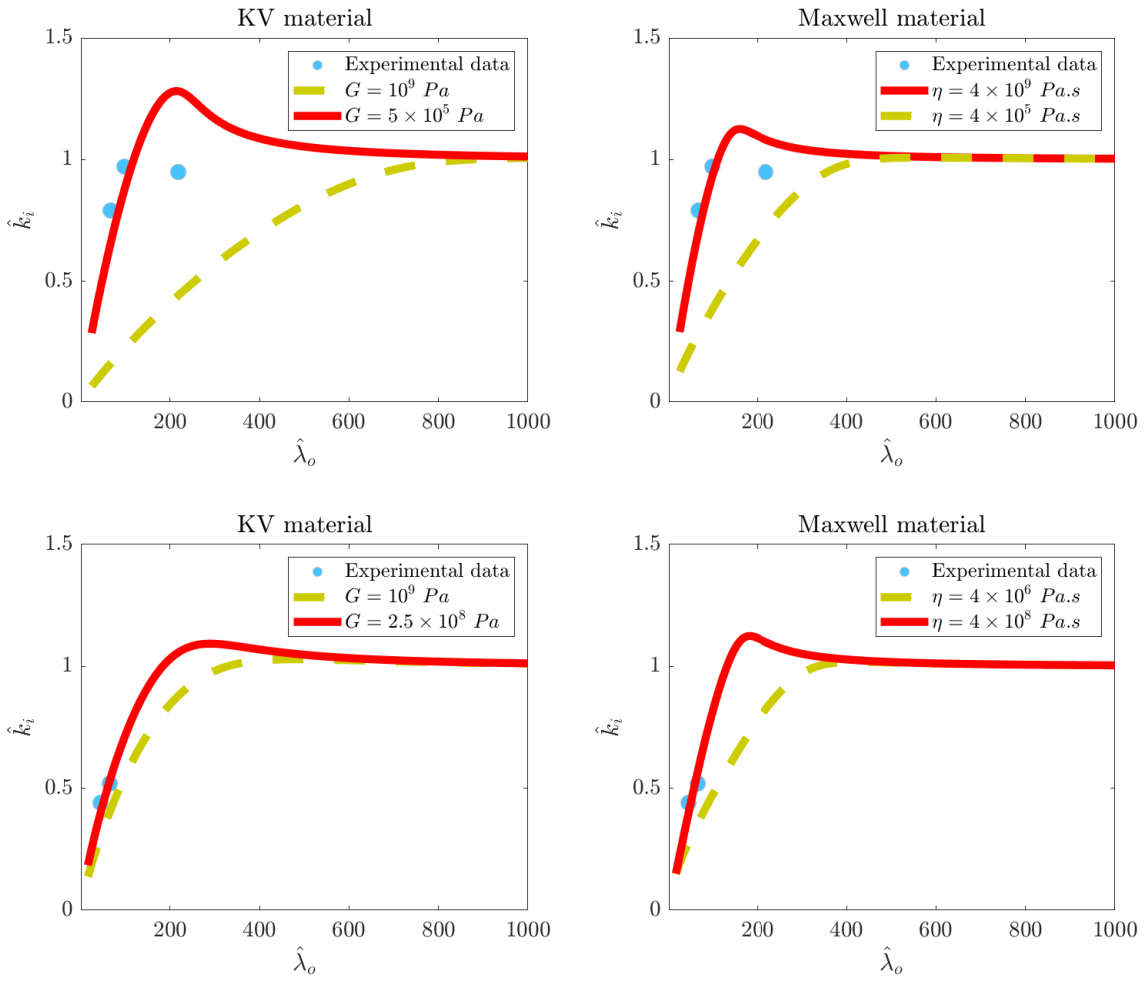

Figure 10. Comparison between $\hat{k}_i$ vs. $\hat{\lambda}_o$ curves predicted by wet beam models and the data measured by Yiew et al. (2019). Upper and lower rows show the data related to freshwater ice covers with thicknesses of 1 cm and 1.5 cm, respectively.

process, though the large difference between inputs giving the best fit for the decay rate and dispersion plots still leaves us with a big question mark about the main reason for such a difference.

As discussed, other researchers have hypnotized that the effective elasticity or dynamic viscosity of the wet ice interacting with water waves can be different from what have been measured in dry tests. While the whole paper looks into ability of KV, Maxwell and pure elastic materials and discusses how accurate their results can be, the idea of developing other models by considering various viscoelastic materials rises. We can use the other solid models to evaluate whether Young Modulus giving the best result for decay rates and dispersion process match with what is found in dry tests or not.

https://doi.org/10.5194/tc-2022-75
Preprint. Discussion started: 9 June 2022

The Cryosphere Discussions
Open Access
EGU

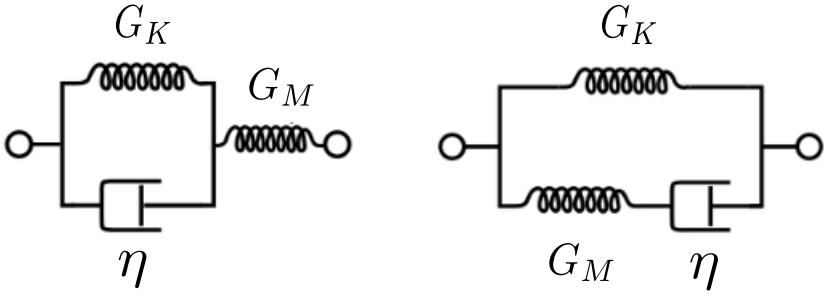

Figure 11. Standard linear solid models. Left and right panels respectively show the SLS KV and SLS Maxwell models.

To provide an answer to the above question, the linear combination of KV and Maxwell materials, known as Standard Linear Solid (SLS) model, is used to describe the mechanical behaviour of ice. Standard Linear Solid models are also called "Zener". Two different Zener models have been introduced in this paper. The first one is a SLS model established using a Kelvin approach (Spring in series with KV). The other model is acquired employing a Maxwell approach (Spring in parallel with Maxwell). The schematic of both of these models are shown in Figure 11. The storage and loss modulii of these two solid models are formulated as

$$G_E = \frac{G_K G_M}{G_K + G_M}\left(G_M + \frac{G_K G_M}{G_K + G_M}\right)\frac{(\omega\tau)^2}{1+(\omega\tau)^2} - i\left(G_M + \frac{G_K G_M}{G_K + G_M}\right)\frac{(\omega\tau)}{1+(\omega\tau)^2}, \tag{24}$$

$$G_E = G_K + \frac{G_M\left(\tau^2\omega^2\right)}{(1+\tau^2\omega^2)} - i\frac{G_M(\tau\omega)}{(1+\tau^2\omega^2)}. \tag{25}$$

The same way used to establish dispersion relationships in the Section 2 is applied, and the related dispersion relationships are formulated as

$$\omega^2 = \left(\frac{\frac{G_K G_M}{G_K+G_M}\left(G_M+\frac{G_K G_M}{G_K+G_M}\right)\frac{(\omega\tau)^2}{1+(\omega\tau)^2}h^3}{6(1-\nu)\rho_w}k^4 - i\frac{\left(G_M+\frac{G_K G_M}{G_K+G_M}\right)\frac{(\omega\tau)}{1+(\omega\tau)^2}\Big)h^3}{6(1-\nu)\rho_w}k^4 + g - i\omega\frac{B}{\rho_w} - \frac{\rho_i(h+A)}{\rho_w}\omega^2\right)k\tanh(kD), \tag{26}$$

$$\omega^2 = \left(\frac{(G_K + \frac{G_M\left(\tau^2\omega^2\right)}{(1+\tau^2\omega^2)})h^3}{6(1-\nu)\rho_w}k^4 - i\frac{\left(\frac{G_M(\tau\omega)}{(1+\tau^2\omega^2)}\right)h^3}{6(1-\nu)\rho_w}k^4 + g - i\omega\frac{B}{\rho_w} - \frac{\rho_i(h+A)}{\rho_w}\omega^2\right)k\tanh(kD). \tag{27}$$

Decay rates and dispersion of waves propagating into the $1.5\ cm$ freshwater ice cover are recalculated by using the two introduced SLS models and plotted in Figure 12. The Left and right panels respectively show the results found using SLS KV and SLS Maxwell models. Dispersion curves are plotted in upper panels, and the decay rates are illustrated in lower panels. SLS KV and SLS Maxwell model both construct $\hat{k}_i$ vs. $\hat{\lambda}_o$ plots similarly. Interestingly, the equivalent Young Modulus of the SLS KV model is $2.5\times\ 10^4\ Pa$ and that of the SLS Maxwell model is $3.3\times\ 10^9\ Pa$. This confirms that the SLS KV model

https://doi.org/10.5194/tc-2022-75
Preprint. Discussion started: 9 June 2022

which is built using the KV approach can only predict the predicted process with a very low equivalent Young Modulus, which is much smaller than Young Modulus found in dry tests (which is around $2.6 \times 10^9\ Pa$). But the equivalent Young Modulus of the SLS Maxwell model is close to what is found in dry tests. This signifies that the freshwater ice formed in the flume is more likely to behave similarly to a SLS Maxwell material. This can explain the difference between the effective Young Modulus reported in different experimental researches. Researchers who conducted those flume/basin experiments concluded that a lower Young Modulus should be used to calculate the dispersion process of waves propagating into ice when a dispersion equation built on the basis of pure elastic material (or the KV material) is employed. But as observed here, the material is more prone to show a rheological behavior falling in between those of the KV and Maxwell materials, arranged using a Maxwell approach, the equivalent Young Modulus of which is close to what is measured in dry tests.

The decay rates are seen to be well predicted by both models. The interesting point is that, the KV model was found not be able to construct the decay rates of $1.5\ cm$ thick. But as seen here, the results of SLS KV model fairly agree with experimental measurements. The SLS Maxwell model can predict the decay rate very well. The trend of the decay rates given by SLS Maxwell and SLS KV are very similar.

3.5 Final discussion

Decay rates and dispersion curves of gravity waves propagating into an ice cover can be constructed using the presented wet beam models. With the same setups (e.g. dynamic viscosity and Young Modulus), different models can give different curves for the decay rates and the dispersion process. Thus, the choice of the model for the prediction of the decay rates and the dispersion process is very important. This needs a better understanding of the ice mechanics and the way it is formed. Simply stated, the mechanics of ice is a very complicated field of research, with lots of open questions not have been answered yet.

Models formulated in the present research follow the basic of the Euler-Bernoulli beam theory, which describes displacements of a solid layer by assuming small motions. To provide a clear picture of this theory, transverse sections of a beam flexed due to an external/internal load should be assumed. If the displacement field follows the Euler-Bernoulli law, the normal vector of any transverse section is always parallel to the axis of the beam. That is, no local rotational motion occurs. This is different from what happens for a solid body following the Timoshenko–Ehrenfest beam theory, where rotational motions are taken into consideration (Timoshenko and Woinowsky-Krieger, 1959). Furthermore, to establish any model, the mechanical behaviour of a substance should be formulated. It left us with two general choices as we are following a beam theory: The ice can be hypothesized to be either elastic or viscoelastic. When elastic behavior is considered, Hooke's law is utilized to formulate the relationship between the stress and the resulting strain. If viscoelastic behavior is assumed, different linear models can be used. The KV and Maxwell models are commonly used for this aim, the former which represents a viscoelastic solid body, and the latter which represents a mass of viscoelastic fluid.

Using mechanical behavior prescribed for the ice and employing an Euler-Bernoulli equation, dispersion relationships can be formulated. If the ice layer is assumed to be dry and no fluid-solid interaction is taken into account, dispersion relationships for wave motions in dry beams are acquired. If the multi-physical problem is considered, the ice layer is assumed to settle down on the water surface and fluid forces emerge. If the fluid motion is assumed to be linear, three different forces including heave

https://doi.org/10.5194/tc-2022-75
Preprint. Discussion started: 9 June 2022

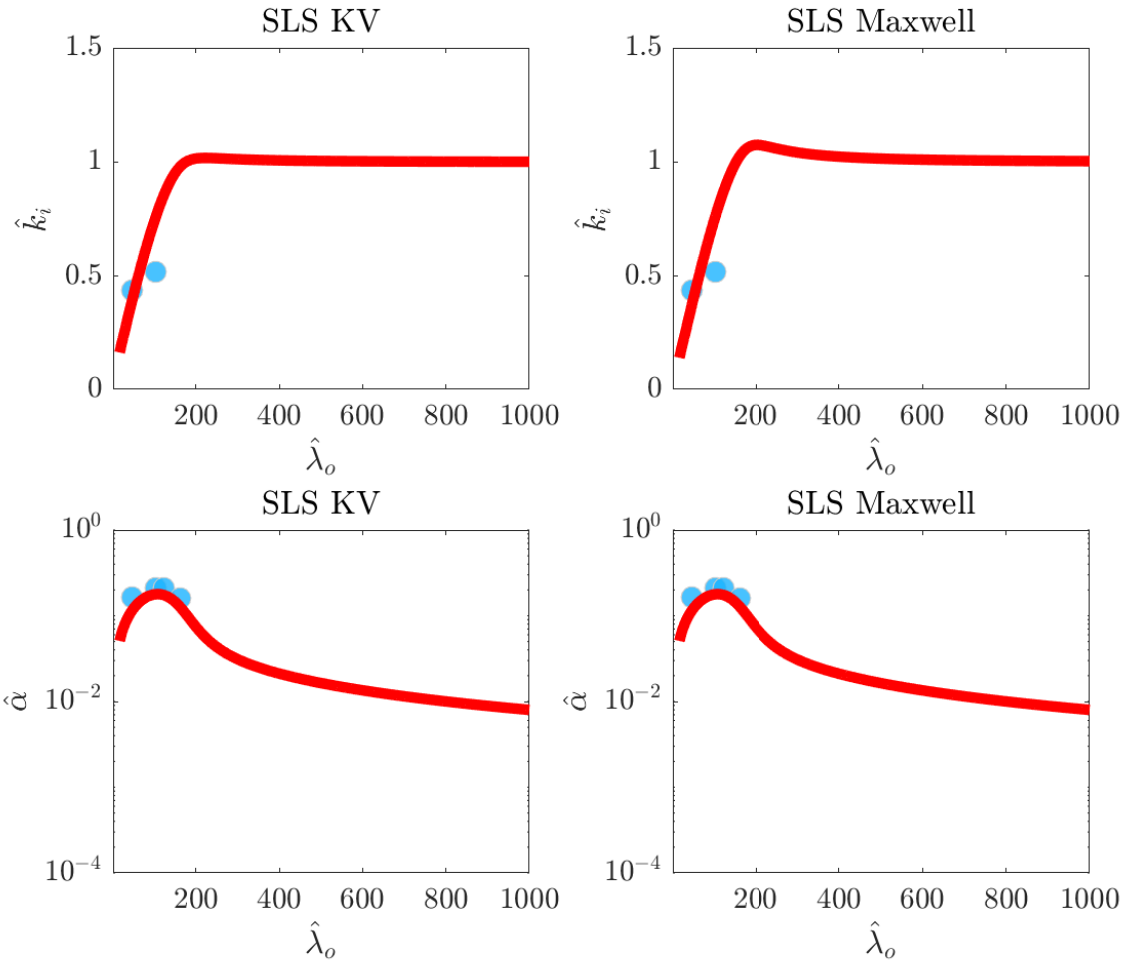

Figure 12. Comparison between predictions of SLS models and values measured byYiew et al. (2019). Upper and lower rows show the decay rates and dispersion plots. Equivalent Young Modulus of the SLS KV model is 2.5×10^4 Pa and equivalent Young Modulus of the SLS Maxwell model is 3.3×10^9 Pa. Dynamic viscosity of SLS KV model is 4×10^7 $Pa.s$ and dynamic viscosity of the SLS Maxwell model is 3.5×10^9 $Pa.s$.

stiffness, heave damping, and heave added mass forces emerge. The original model of Greenhill (1886) and Fox and Squire (1991) models only consider stiffness of fluid, i.e, the dispersion relationship presented by them has one extra term compared to the dispersion relationship of a purely dry elastic beam, which is the stiffness term. The dispersion relationship formulated by Mosig et al. (2015) has included fluid heave damping but only for an elastic material, and the available formulated dispersion relationship of a viscoelastic material with no heave damping. But in reality, fluid heave damping occurs due to wave radiation (which generates added mass and damping forces) and its presence does not have any inconsistency with the viscoelasticity of

https://doi.org/10.5194/tc-2022-75
Preprint. Discussion started: 9 June 2022

the ice. That comes from the basic of marine hydrodynamics where the Radiation Problem is formulated to describe motions of any solid body on the water surface (Newman, 1977). To conclude, a more general dispersion relationship, compared to available ones, can be formulated if three fluid force terms are considered. In the present research, all three fluid forces were considered to formulate the dispersion relationship of a wet layer of ice, covering water.

Energy dissipation is caused by solid-based energy damping and fluid-based energy damping. The former is dominant over high frequencies (corresponding to short waves in an open-water condition), and the latter is dominant over small frequencies (corresponding to long waves in an open-water condition). The solid-based energy damping is caused by the viscoelastic resistance emerging in the solid and is absent for an elastic material. Regardless of the viscoelastic model used to treat the mechanical behavior of the material, the solid-based energy damping decreases with an increase in the wavelength. With an increase in Elasticity number, the wavelength range over which solid-based energy damping is dominant becomes wider. This matches with physics. The body is more rigid and solid responses can contribute to energy damping of longer waves, compared to bodies with low rigidity. The fluid-based energy dissipation is generated by radiation forces, decreasing with the increase in wavelength. But compared to the solid-based energy damping, the rate of decrease is much smaller. The energy damping triggered by a pure elastic cover is only due to the presence of heave damping forces. Thus, to compensate for the lack of solid-based energy damping of an elastic cover, larger heave damping needs to be considered. Energy decay triggered by the landfast ice covers which have large rigidity can be computed using the viscoelastic models if fluid heave damping is included. If it is not, models cannot work properly and the predicted decay curves diverge from field measurements. This well confirms that fluid-based energy damping contributes to total energy dissipation. Both viscoelastic models were seen to construct the decay curves, fairly follow field measurements. But the dynamic viscosity values were seen to be much different. A KV material may be a more realistic indicator of ice behavior as the lanfast ice is expected to be solid.

Decay rates of broken ice fields were seen to be calculated by both viscoelastic models when the fluid-based energy damping is considered. This provided us with another piece of evidence for the contribution of heave forces to energy dissipation. Compared to landfast ice covers, different values of the dynamic viscosity were observed to give the best fitting for the decay rates of waves advancing in water partially covered with broken ice floes. The coexistence of open-water and ice floes on the upper layer of the fluid domain can explain this. Models are formulated for an integrated layer of solid ice. If water is included, a mixed thin layer represents the cover. A volume fraction model may describe the dynamic viscosity of the layer. The dynamic viscosity of the water is much smaller compared to that of ice, but the water entrapped between ice floes may be turbulent, leading to eddy generation (turbulent flow can cause damping of waves, *e.g.* Tavakoli et al. (2022)). The KV model gives the best fitting of decay rate when the dynamic viscosity is reduced, compared to the landfast ice. In contrast, the Maxwell model gives the best fitting with a larger dynamic viscosity. Thus, what can be concluded is that if water reduces the dynamic viscosity of the upper layer, the KV model will more likely to be a better indicator of the ice behavior. Otherwise, the Maxwell model prescribes the mechanical behaviour of the material.

The decay rates of the freshwater ice were also calculated. The pure elastic materials can reconstruct the decay rates only if a very large heave damping is used, which may not be realistic. But, viscoelastic models were seen to predict the decay rate plots. Models, however, were not able to capture the dispersion process under freshwater ice covers with the same input observed to

https://doi.org/10.5194/tc-2022-75
Preprint. Discussion started: 9 June 2022

give the best decay rates. Effective values were seen to construct dispersion plots with an acceptable level of accuracy. This has been observed and reported by other scholars over the last two decades, who measured the wavelength and phase speed of disintegrated elastic/viscoelastic covers. The interesting point is that, when a Maxwell model is used, the dynamic viscosity can affect the dispersion process. This motivates us to build other models which formulate the storage modulus by applying the dynamic viscosity. Two available linear models were introduced. One is SLS KV and the other is SLS Maxwell. Both models include two springs and one dashpot. The equivalent Young Modulus giving the best fitting when SLS KV is used is 2.5×10^4 Pa, which is much smaller compared to that of real freshwater ice. But, for SLS Maxwell, the equivalent Young Modulus was seen to be 3.3×10^9 Pa which is close to that of freshwater ice.

Based on what was observed when SLS models were used, it can be concluded that simple models such as Maxwell and KV, cannot reproduce behavior of the freshwater ice formed in the flume, and its behavior is different from that of the landfast ice. There are still doubts about the behaviour of broken sea ice. Both Maxwell and KV models were found to give the best fitting. One reason is that the wave phase is not measured in most of the field tests that took place in the broken ice field, and researchers were mostly concerned with decay rates. Since the phase speed and dispersion plots are not available, the performance of models in the reconstruction of dispersion plots cannot be evaluated. Especially, this could show whether changes in the dynamic viscosity can modify the accuracy of the Maxwell model in the prediction of dispersion or not (dispersion curves Maxwell model give is sensitive to dynamic viscosity). That may be still an open question for the future.

4 Conclusions

The common approach used to predict decay rates and dispersion of waves passing through an ice cover is to formulate a dispersion relationship, the roots of which give the decay rate and the relative wavenumber in an ice-covered sea. The majority of models developed for wave-ice interaction have been developed based on two approaches. First, ice was assumed to be a viscous fluid or a viscoelastic solid layer. Second, ice was assumed to be elastic, and the fluid forces were taken into account. This paper aimed to present wet beam models by considering both of fluid-based and solid-based energy dissipation mechanisms by accommodating different rheological for the ice layer (KV, Maxwell, and pure elastic materials). Thus the models were called “wet beam” which refers to water-based forces that are taken into consideration.

Predictions of models and field measurements were quantitatively compared against each other. KV and Maxwell models were seen to reconstruct the decay rates and dispersion process of landfast ice with a great level of accuracy. Decay rates were observed to be poorly predicted if the fluid-based energy damping is not taken into account, suggesting that this mechanism has a very important role in ice-induced energy decay over the range of long waves. The decay rates of unconsolidated ice fields were also seen to be accurately predicted by KV and Maxwell models by setting a non-zero value for the fluid damping coefficient.

Decay rates and wave dispersion of freshwater ice were predicted. The pure elastic model was seen to predict the decay rate with an unrealistic heave fluid damping. The decay rates predicted by KV and Maxwell models were seen to agree with experiments, though the dispersion plots were observed to diverge from the experimental data.

https://doi.org/10.5194/tc-2022-75
Preprint. Discussion started: 9 June 2022

Two standard linear solid models were used and two other dispersion relationships were formulated. These relationships were seen to predict the attenuation rate and the dispersion plots with a good level of accuracy. But, the SLS model which was fundamentally based on the KV material gave the best fitting with an unrealistic Young Modulus.

Overall, the wet beam dispersion relationships developed by accommodating two-parameter solid models are able to predict the decay rates and dispersion process of ice fields. But, for freshwater ice flume, a three-parameter solid model may increase the accuracy of the predictions. In the future, nonlinear models can also be developed to consider the effects of wave steepness, and other beam theories can be employed.

Code availability. The code used for construction of the curves can be provided upon reasonable request.

Data availability. This paper does not use any dataset. All the experimental data were extracted from Figures or Tables of other references listed in Table 1 (Voermans et al. (2021); Wadhams et al. (1988); Meylan et al. (2014); Yiew et al. (2019); Sree et al. (2018)).

Video supplement. This research does not include any supplementary file.

Author contributions. ST and AVB conceptualized the research. AVB supervised the research and provided the funding. ST formulated the models and visualized the data. ST and AVB discussed the results. ST wrote the draft of the paper. AVB reviewed the paper.

Competing interests. The authors declare that they have no known competing financial interests or personal relationships that could have appeared to influence the work reported in this paper.

Acknowledgements. ST was supported by a Melbourne Research scholarship. AVB acknowledges support through the US ONR and ONRG Grant Number N62909-20-1-2080.

https://doi.org/10.5194/tc-2022-75
Preprint. Discussion started: 9 June 2022

References

Cheng, S., Tsarau, A., Evers, K.-U., and Shen, H.: Floe Size Effect on Gravity Wave Propagation Through Ice Covers, Journal of Geophysical Research: Oceans, 124, https://doi.org/10.1029/2018JC014094, 2019.

Collins, C., Rogers, W., and Lund, B.: An investigation into the dispersion of ocean surface waves in sea ice, Ocean Dynamics, 67, https://doi.org/10.1007/s10236-016-1021-4, 2016.

Comiso, J., Parkinson, C., Gersten, R., and Stock, L.: Comiso JC, Parkinson CL, Gersten R, Stock L.. Accelerated decline in the Arctic sea ice cover. Geophys Res Lett 35: L01703, Geophysical Research Letters, 35, 1703–, https://doi.org/10.1029/2007GL031972, 2008.

De Carolis, G. and Desiderio, D.: Dispersion and attenuation of gravity waves in ice: a two-layer viscous fluid model with experimental data validation, Physics Letters A, 305, 399–412, https://doi.org/https://doi.org/10.1016/S0375-9601(02)01503-7, 2002.

Fox, C. and Squire, V. A.: Coupling between the ocean and an ice shelf, Annals of Glaciology, 15, 101–108, https://doi.org/10.3189/1991AoG15-1-101-108, 1991.

Greenhill, A. G.: Wave Motion in Hydrodynamics, American Journal of Mathematics, 9, 62–96, http://www.jstor.org/stable/2369499, 1886.

Herman, A., Cheng, S., and Shen, H. H.: Wave energy attenuation in fields of colliding ice floes – Part 1: Discrete-element modelling of dissipation due to ice–water drag, The Cryosphere, 13, 2887–2900, https://doi.org/10.5194/tc-13-2887-2019, 2019.

Huang, L., Ren, K., Li, M., Željko Tuković, Cardiff, P., and Thomas, G.: Fluid-structure interaction of a large ice sheet in waves, Ocean Engineering, 182, 102–111, https://doi.org/https://doi.org/10.1016/j.oceaneng.2019.04.015, 2019.

Jain, M. and Mehta, A. J.: Role of basic rheological models in determination of wave attenuation over muddy seabeds, Continental Shelf Research, 29, 642–651, https://doi.org/https://doi.org/10.1016/j.csr.2008.09.008, on the dynamics of mud deposits in coastal areas, 2009.

Kohout, A., Williams, M., Dean, S., and Meylan, M.: Storm-induced sea-ice breakup and the implications for ice extent, Nature, 509, 604–7, https://doi.org/10.1038/nature13262, 2014.

Lamb, H.: Hydrodynamics, 1932.

Langleben, M. P.: YOUNG'S MODULUS FOR SEA ICE, Canadian Journal of Physics, 40, 1–8, https://doi.org/10.1139/p62-001, 1962.

Liu, A. K. and Mollo-Christensen, E.: Wave Propagation in a Solid Ice Pack, Journal of Physical Oceanography, 18, 1702 – 1712, https://doi.org/10.1175/1520-0485(1988)018<1702:WPIASI>2.0.CO;2, 1988.

Liu, Q., Rogers, W., Babanin, A., Li, J., and Guan, C.: Spectral Modeling of Ice-Induced Wave Decay, Journal of Physical Oceanography, 50, https://doi.org/10.1175/JPO-D-19-0187.1, 2020.

Marchenko, A., Haase, A., Jensen, A., Lishman, B., Rabault, J., Evers, K.-U., Shortt, M., and Thiel, T.: Laboratory Investigations of the Bending Rheology of Floating Saline Ice and Physical Mechanisms of Wave Damping in the HSVA Hamburg Ship Model Basin Ice Tank, Water, 13, https://www.mdpi.com/2073-4441/13/8/1080, 2021.

Meier, W. N., Gallaher, D., and Campbell, G. G.: New estimates of Arctic and Antarctic sea ice extent during September 1964 from recovered Nimbus I satellite imagery, The Cryosphere, 7, 699–705, https://doi.org/10.5194/tc-7-699-2013, 2013.

Meylan, M., Bennetts, L., and Kohout, A.: In-situ measurements and analysis of ocean waves in the Antarctic marginal ice zone, Geophysical Research Letters, 41, https://doi.org/10.1002/2014GL060809, 2014.

Mosig, J., Montiel, F., and Squire, V.: Comparison of viscoelastic-type models for ocean wave attenuation in ice-covered seas, Journal of Geophysical Research: Oceans, 120, https://doi.org/10.1002/2015JC010881, 2015.

Newman, J. N.: Marine Hydpdynamics, MIT Press, Massachusetts, US, 1977.

Parra, S. M., Sree, D. K., Wang, D., Rogers, E., Lee, J. H., Collins, C. O., Law, A. W.-K., and Babanin, A. V.: Experimental study on surface wave modifications by different ice covers, Cold Regions Science and Technology, 174, 103 042, https://doi.org/https://doi.org/10.1016/j.coldregions.2020.103042, 2020.

Robin, G.: Wave propagation through fields of pack ice, Philosophical Transactions of the Royal Society of London. Series A, Mathematical and Physical Sciences, 255, 313–339, https://doi.org/10.1098/rsta.1963.0006, 1963.

Robinson, N. and Palmer, S.: A modal analysis of a rectangular plate floating on an incompressible liquid, Journal of Sound and Vibration, 142, 453–460, https://doi.org/https://doi.org/10.1016/0022-460X(90)90661-I, 1990.

Rogers, W. and Orzech, M.: Implementation and testing of ice and mud source functions in WAVEWATCH III, 2013.

Sakai, S. and Hanai, K.: Empirical formula of dispersion relation of waves in sea ice, Ice in the Environment: Proceedings of the 16th IAHR International Symposium on Ice, 2, 2002.

Serra-Aguila, A., Puigoriol, J., Reyes, G., and Menacho, J.: Viscoelastic models revisited: characteristics and interconversion formulas for generalized Kelvin-Voigt and Maxwell models, Acta Mechanica Sinica, 35, 1191–1209, https://doi.org/10.1007/s10409-019-00895-6, 2019.

Squire, V.: Of ocean waves and sea-ice revisited, Cold Regions Science and Technology, 49, 110–133, https://doi.org/https://doi.org/10.1016/j.coldregions.2007.04.007, 2007.

Squire, V. and Allan, A.: Propagation of flexural gravity waves in sea ice, in: Sea Ice Processes and Models, Prec. Arctic Ice Dynamics Joint Experiment Commission of Snow and Ice, Symposium, pp. 327–338, Univ. of Washington Press, Reykjavík, Iceland, 1977.

Squire, V. A.: Ocean Wave Interactions with Sea Ice: A Reappraisal, Annual Review of Fluid Mechanics, 52, 37–60, https://doi.org/10.1146/annurev-fluid-010719-060301, 2020.

Squire, V. A., Dugan, J. P., Wadhams, P., Rottier, P. J., and Liu, A. K.: Of Ocean Waves and Sea Ice, Annual Review of Fluid Mechanics, 27, 115–168, https://doi.org/10.1146/annurev.fl.27.010195.000555, 1995.

Sree, D. K., Law, A. W.-K., and Shen, H. H.: An experimental study on gravity waves through a floating viscoelastic cover, Cold Regions Science and Technology, 155, 289–299, https://doi.org/https://doi.org/10.1016/j.coldregions.2018.08.013, 2018.

Stroeve, J., Serreze, M., Drobot, S., Gearheard, S., Holland, M., Maslanik, J., Meier, W., and Scambos, T.: Arctic Sea Ice Extent Plummets in 2007, Eos, Transactions American Geophysical Union, 89, https://doi.org/10.1029/2008EO020001, 2008.

Sutherland, G., Halsne, T., Rabault, J., and Jensen, A.: The attenuation of monochromatic surface waves due to the presence of an inextensible cover, Wave Motion, 68, https://doi.org/10.1016/j.wavemoti.2016.09.004, 2016.

Tavakoli, S., Niazmand Bilandi, R., Mancini, S., De Luca, F., and Dashtimanesh, A.: Dynamic of a planing hull in regular waves: Comparison of experimental, numerical and mathematical methods, Ocean Engineering, 217, 107 959, https://doi.org/https://doi.org/10.1016/j.oceaneng.2020.107959, 2020.

Tavakoli, S., Shaghaghi, P., Mancini, S., De Luca, F., and Dashtimanesh, A.: Wake waves of a planing boat: An experimental model, Physucs of Fluids, 34, 037 104, https://doi.org/10.1063/5.0084074, 2022.

Timoshenko, S. and Woinowsky-Krieger, S.: Theory of Plates and Shells, Engineering mechanics series, McGraw-Hill, 1959.

Voermans, J. J., Liu, Q., Marchenko, A., Rabault, J., Filchuk, K., Ryzhov, I., Heil, P., Waseda, T., Nose, T., Kodaira, T., Li, J., and Babanin, A. V.: Wave dispersion and dissipation in landfast ice: comparison of observations against models, The Cryosphere, 15, 5557–5575, https://doi.org/10.5194/tc-15-5557-2021, 2021.

Wadhams, P.: Measurement of wave attenuation in pack ice by inverted echo sounding, in: Proceedings of the International Sea Ice Conference, pp. 255–260, Nat. Res. Counc. of Iceland, Reykjavík, Iceland, 1972.

https://doi.org/10.5194/tc-2022-75
Preprint. Discussion started: 9 June 2022

565 Wadhams, P., Squire, V. A., Goodman, D. J., Cowan, A. M., and Moore, S. C.: The attenuation rates of ocean waves in the marginal ice zone, Journal of Geophysical Research, 93, 6799–6818, 1988.

Wang, R. and Shen, H.: Gravity waves propagating into an ice-covered ocean: A viscoelastic model, Journal of Geophysical Research, 115, 1–12, https://doi.org/10.1029/2009JC005591, 2010.

Yiew, L., Parra, S., Wang, D., Sree, D., Babanin, A., and Law, A.-K.: Wave attenuation and dispersion due to floating ice covers, Applied
570 Ocean Research, 87, 256–263, https://doi.org/https://doi.org/10.1016/j.apor.2019.04.006, 2019.

Young, I., Zieger, S., and Babanin, A.: Global Trends in Wind Speed and Wave Height, Science (New York, N.Y.), 332, 451–5, https://doi.org/10.1126/science.1197219, 2011.

Yu, J., Rogers, W. E., and Wang, D. W.: A Scaling for Wave Dispersion Relationships in Ice-Covered Waters, Journal of Geophysical Research: Oceans, 124, 8429–8438, 2019.

575 Zhao, X. and Shen, H. H.: Ocean wave transmission and reflection between two connecting viscoelastic ice covers: An approximate solution, Ocean Modelling, 71, 102–113, https://doi.org/https://doi.org/10.1016/j.ocemod.2013.04.002, arctic Ocean, 2013.